Original Article

Qualitative and Quantitative Study of the Changes in the Ultrastructure of Mammalian Adrenal Cortex Caused by the Venezuelan Tigra Mariposa (*Bothrops venezuelensis*) Snake Venom

Héctor J Finol, Estefanie Garcia-Lunardi, Roschman González, Maria E Girón[1], Nestor L Uzcátegui[1], Alexis Rodríguez-Acosta[1]

Microscopy Electronic Centre, Faculty of Sciences, Universidad Central De Venezuela, Caracas, Venezuela, [1]Anatomical Institute, Immunochemistry and Ultrastructure Laboratory, Universidad Central De Venezuela, Caracas, Venezuela

Abstract

The damage of the adrenal gland by snake venoms needs to be clarified. Lethality (LD_{50}) of *Bothrops venezuelensis (Bv)* venom was established by intraperitoneally mice injections. Preparation of specimens for transmission electron microscopy samples from cortex adrenal gland biopsies at 3, 6, and 24 h was processed. The quantitative description by the principal component analysis (PCA) of the adrenal gland was as follows: thickening of the capillary endothelium, area of the capillary lumen, cell nucleus area, enlargement of the perinuclear space, number of mitochondria, area of the mitochondria, number of mitochondrial cristae, number of cristae per mitochondrial unit, and tubular diameter of the smooth endoplasmic reticulum (SER). Sections of the adrenal cortex, after 3 h postinjection with *Bv* venom showed in the cortical cells: mitochondria with tubular cristae and slightly swollen SER cisternae, nucleus with variable heterochromatin content, irregular edges, and swollen nuclear envelope. After 6 h, cells with swollen nucleus envelope, electron dense lipids and mitochondria with loss of their cristae were observed. Myelin figures, close to the microvilli of the cortical cell, multivesicular bodies, swollen profiles of the SER, and electron dense lipid drops were noticed. After 24 h, thickening of the endothelial wall, fenestrae and projections into the capillary lumen, loss of the mitochondrial cristae, destruction of the capillary and the plasma membrane of the cortical cell, multivesicular body, SER loss, and an enlargement of the perinuclear space were detected. In the quantitative PCA, there were significant changes after the venom treatments.

Keywords: Adrenal gland, *Bothrops venezuelensis*, mitochondria, principal component analysis, smooth endoplasmic reticulum, ultrastructure, venom

Introduction

Hemostasis disorders and organ damages by proteolytic action are the main signs of envenoming by *Bothrops* snake venoms.[1-6] The snake venom proteases have been related to the pathogeny of the adrenal gland injuries.[7-16]

Bothrops venezuelensis (Bv) venom effects[3] were carried out covering the first 24 h, obtaining samples from the adrenal gland cortex of injected mice at 3, 6, and 24 h.

In the present work, a group of subcellular changes were showed, which could explain the pathophysiological alterations concerning the adrenal gland caused by *Bv* venom.

Received: 18-08-2019 **Accepted:** 09-05-2020 **Published:** 10-09-2020

Access this article online

Quick Response Code:

Website: http://www.jmau.org/

DOI: 10.4103/JMAU.JMAU_49_19

Materials and Methods

Snakes

The "tigra mariposa" *Bv* snakes were obtained from the Waraira Repano mountains, at North of Caracas city (Bolivarian Republic of Venezuela), a typical subtropical rain forest, with average temperatures of 25°C, annual rainfall

Address for correspondence: Dr. Alexis Rodríguez-Acosta, Immunochemistry and Ultrastructure Laboratory, Anatomical Institute, Universidad Central De Venezuela, Caracas, Venezuela.
E-mail: rodriguezacosta1946@yahoo.es

How to cite this article: Finol HJ, Garcia-Lunardi E, González R, Girón ME, Uzcátegui NL, Rodriguez-Acosta A. Qualitative and quantitative study of the changes in the ultrastructure of mammalian adrenal cortex caused by the venezuelan tigra mariposa (*Bothrops venezuelensis*) snake venom. J Microsc Ultrastruct 2020;8:104-14.

of 1500–2000 mm, and atmospheric humidity superior than 80%.[17] Six both sexes' snakes were located and maintained at the Serpentarium of the Tropical Medicine Institute of the Universidad Central de Venezuela (Caracas, Venezuela).

Venom collection

Venom was achieved by permitting the snakes to bite into a Para-film® stretched over a disposable plastic cup. The venom samples were centrifuged (500×g for 15 min) and filtered through 0.45 μm filter under positive pressure. The venom was frozen at − 80°C, lyophilized, and maintained at −30°C until used. Sublethal (5.0 mg/kg) samples of reconstituted venom were prepared for the experimental injection of mice.

Mice

Ultrastructural adrenal gland studies were performed using NIH mice (18–22 g) purchased from the vivarium, of the National Institute of Hygiene "Rafael Rangel," Caracas, Venezuela. Animals were supplied with water and food *ad libitum* until used.

Ethical statement

Qualified staff controlled all the experimental methods relating to the use of live animals. Applicable regulations as well as institutional guidelines, according to the protocols approved by the Institute of Anatomy Ethical Committee of the Universidad Central de Venezuela, on March 7, 2018, under assurance number 07-03-18. The research was carried out in accordance with the U. K. Animals (Scientific Procedures) Act, 1986 and associated guidelines, EU Directive 2010/63/EU for animal experiments.

Lethal activity

Lethality of *Bv* venom was established by intraperitoneally injections into mice, and the LD_{50} calculation was done, according to the method of Spearman-Kärber.[18] Six groups containing five mice were injected (0.2 mL) intraperitoneally, with different venom concentrations (4.0–7.0 mg/kg) diluted in phosphate-buffered saline (PBS) solution. An equivalent volume of PBS was injected as a negative control group. The animals were observed for 48 h after injections.

Preparation of specimens for electron microscopy

Three adult male NIH strain mice (normal control group) were injected intravenously (IV) in the tail vein with 0.1 mL of PBS solution. Nine mice (experimental group) were injected IV with 5.0 mg/kg of *Bv* in 100 μL of PBS. After 3, 6, and 24 h, three mice from each group were ready for adrenal gland biopsies. The fragments were instantly obtained, from control and experimental mice, after to be euthanized by cervical dislocation. The samples were without delay *in situ* fixed with 3% glutaraldehyde and then with 1% OsO4 (both fixatives diluted in 320 mM phosphate buffer saline, pH 7.4), dehydrated in ethanol, and embedded in LX-112 resin (Ladd Research Inc.). Ultrathin sections were stained with uranyl acetate and lead citrate. At that point, observed with an FEI, Tecnai Spirit 12G2 model transmission electron microscope, with an accelerating voltage of 100 kV.

Digitization of the image

For the descriptive study of the biological systems from a micrograph, the magnification used for their registration was considered, as well as the magnification factor, with which the revealed physical image was obtained. Using the "mouse," we could delineate points, the length, the angle, the area, etc., in the image taken directly from the TEM so that the object in the image could be established in real time. Thus, the images acquired directly from the electron microscope were used to the quantitative study. The structures measured with the TEM were processed with the computer to analyze and classify the data using statistical programs. They were included and maintained the size according to the original magnification, with which it was achieved. The images obtained by the FEI Quanta 250 FEG equipment were stored digitally in a computer for further study.

Calculated usage of the results

ImagineJ

From the micrographs acquired in the thin and thick sections, morphometric magnitudes were carried out through the IMAGEJ program.

Principal component analysis

The principal component analysis (PCA) consisted of expressing a set of variables in a set of linear combinations of factors, which are not correlated among them. This process permitted to symbolize the original data (individuals and variables) in a space of fewer dimensions than the original space. The assessed variables for the quantitative description of the adrenal gland were thickening of the capillary endothelium, area of the capillary lumen, cell nucleus area, swelling of the perinuclear space, number of the mitochondria, area of the mitochondria, number of mitochondrial cristae, number of cristae per mitochondrial unit, and tubular diameter of the smooth endoplasmic reticulum (SER).

Statistical analysis

ANOVA is a statistical procedure that uses the analysis of variance, which allows examining, if more than two groups diverge significantly among themselves, in terms of their means and variances. Classically, the ANOVA is used to associate a probability, with the assumption that the mean of a group of scores is different from the mean of another group of scores. Through the comparison, it was attempted to test a hypothesis of difference between more than two groups.[19]

Smallest statistically detectable difference test

It was carried out comparing the statistical values obtained by *Bv* venom treatment with those obtained in the normal control group treatment. The letters a, b, c, d, e, f, and g are derived from a *posteriori* smallest statistically detectable difference (SDD) test.[20]

Results

Lethal activity of *Bothrops venezuelensis* venom

The lethal activity of *Bv* venom expressed as LD_{50} was 6.4 mg/kg.

Adrenal gland changes induced by *Bothrops venezuelensis* venom analyzed by transmission electron microscopy

In the adrenal gland cortex normal control, the mitochondria were observed with their tubular cristae, central nuclei with the normal nuclear envelope, associated with heterochromatin, rough endoplasmic reticulum (RER) short cisternae, tubular profiles of the SER, Golgi (Go) reticular apparatus, lipofuscin granules in different stages of growth (triangle), capillary microvilli (oval), and a lipid drop (Lip) [Figure 1].

The adrenal gland cortex after 3 h of *Bv* venom injection showed loss of the continuity of the endothelial wall, projections into the capillary lumen, and remains of the endothelial wall (the plasma membrane was not distinguished). There was a larger space between the limit of the endothelial cell and the cortical cell. In the cortical cell, the round and slightly elongated profiles corresponded to the SER tubules. Swollen mitochondria with scarce cristae were observed [Figure 2a].

In the cortical cell, a nucleus of irregular contours with abundant heterochromatin and the enlargement of the perinuclear space was noticed. There was a Golgi apparatus, clearly swollen mitochondria, very swollen cisternae of RER, and an autophagic vacuole, with mitochondrial debris [Figure 2b].

Circular profiles of different diameters corresponded to cross-sections of SER. Mitochondria with tubular cristae were also observed [Figure 2c].

Lipid droplets of different electron densities and swollen mitochondria were noticed. Adjacent to the mitochondria, a lipofucsin granule was seen. Circular profiles and small tubules of SER were observed. There were also profiles of larger diameter [Figure 2d].

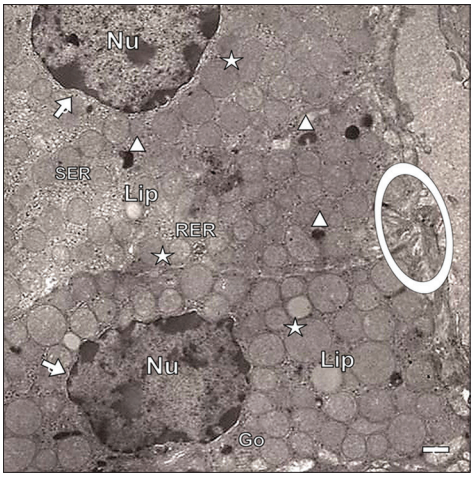

Figure 1: The adrenal gland cortex normal control. The mitochondria are observed with the tubular cristae (star), central nuclei (Nu) with normal perinuclear space (arrow) associated with heterochromatin, short cisternae of the rough endoplasmic reticulum, tubular profiles of the smooth endoplasmic reticulum, Golgi (Go), lipofuscin granules in different stages of growth (triangle), capillary microvilli (oval), and a lipid drop (Lip). Micromark = 1 μm

The adrenal gland cortex after 6 h of *Bv* venom injection showed a fibroblast with an elongated nucleus and an enlargement of the perinuclear space, which lies between the plasma membrane of the cortical cell and the capillary wall where the fenestra was noticed. Swollen cisternae of the RER were detected. The separation of the plasma membrane from the cortical cell and the fibroblast was seen. A mitochondrion with tubular ridges and a lipid drop was also observed [Figure 3a].

A pseudoinclusion of the cytoplasm was seen, surrounded by a nuclear envelope and the nuclear side; besides heterochromatin was noticed [Figure 3b].

A very electron dense lipid drop and a myelin figure were seen. The microvilli of the cortical cell and the mitochondria were

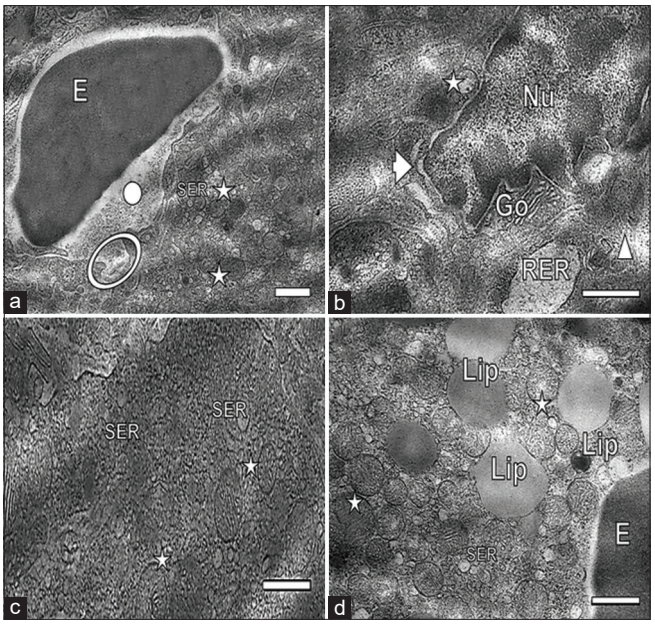

Figure 2: Adrenal gland cortex after 3 h of *Bothrops venezuelensis* venom injection. (a) An erythrocyte is observed within the capillary (E), loss of the continuity of the endothelial wall (oval), projections of the capillary lumen and remains of the endothelial wall (the plasma membrane is not distinguished) (circle). The longer oval indicates a larger space between the limit of the endothelial cell and the cortical cell. In the cortical cell, the round and slightly elongated profiles correspond to the smooth endoplasmic reticulum tubular. Swollen mitochondria with scarce cristae (stars) are observed. Micromark = 1 μm. (b) In the cortical cell, a nucleus (Nu) of irregular contours with abundant heterochromatin and dilated perinuclear space (arrowhead) is noticed. There is a Golgi apparatus (Go), a clearly swollen mitochondria (star), a very swollen cisternae of rough endoplasmic reticulum (RER) and an autophagic vacuole with mitochondrial debris (triangle). Micromark = 1 μm. (c) The circular profiles of different diameters correspond to cross-sections of smooth endoplasmic reticulum. Mitochondria with tubular cristae (star) are observed. Micromark = 1 μm. (d) Lipid droplets (Lip) of different electron density are seen; swollen mitochondria (star) where a lipofucsin granule is observed adjacent to the mitochondria. Circular profiles and small tubules of smooth endoplasmic reticulum are seen). There are also profiles of larger diameter. An erythrocyte is located (E). Micromark = 1 μm

appreciated. The profiles of different diameter of SER were observed [Figure 3c].

Mitochondria with swollen cristae, a lipid droplet, profiles of different diameter of SER, and a multivesicular body (MVB) were also seen [Figure 3d].

The adrenal gland cortex after 24 h of *Bv* venom injection, the endothelial wall showed some fenestrae, and there was an area of wall discontinuity. Several lipid drops, profiles of SER, as well as areas lacking of them were noticed. Various swollen mitochondria were seen [Figure 4a].

The destruction of a capillary was observed where the endothelial wall disappeared. A MVB, loss of the SER, and a lysosome were observed [Figure 4b].

The nucleus exhibited some areas of enlargement of the perinuclear space [Figure 4c]. It was observed a nucleus without heterochromatin and an electron dense body that could be the nucleolus, but with its characteristic structure lost (fibrillar center, dense fibrillar component, and granular component). The structure of the perinuclear space was not distinguished, and in the cytoplasm, there was degeneration, with swollen profiles of SER. Mitochondria with swollen cristae were observed [Figure 4d].

The quantitative principal component analyses under *Bothrops venezuelensis* venom activity and smallest statistically detectable difference test

In the statistical values obtained by *Bv* venom treatment, compared with those obtained in the control treatment, there was a significant difference between the results [Table 1]. The letters a, b, c, d, e, f, and g are derived, from a posteriori SDD test,[20] in which the groups, that have significant differences amid their averages [Table 1].

Table 2 shows that principal component (PCA)-1 [X axis of Figure 5] describes 90.89% of the information of the variable system and (PCA)-2 [y axis of Figure 5] 4.9% of this

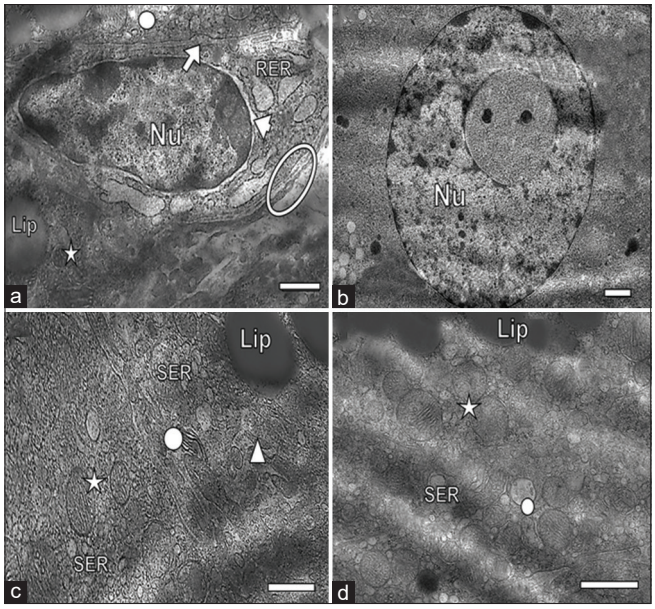

Figure 3: The adrenal gland cortex after 6 h of *Bothrops venezuelensis* venom injection. (a) A fibroblast with an elongated nucleus (Nu) and a swollen perinuclear space (arrow head) which lies between the plasma membrane of the cortical cell (arrow) and the capillary wall where the fenestrae are observed of it (oval). Swollen cisternae of the rough endoplasmic reticulum are observed. Above is seen the separation of the plasma membrane from the cortical cell and the fibroblast (circle). A mitochondrion (star) with tubular cristae and a lipid drop (Lip) is observed. Micromark = 1 μm. (b) A pseudoinclusion of the cytoplasm is seen, surrounded by the perinuclear space and associated to the latter by the nuclear side, heterochromatin is noticed. Micromark = 1 μm. (c) A very electron dense lipid drop (Lip) and a myelin figure (circle) are seen. The microvilli of the cortical cell (triangle) and mitochondria (star) are appreciated. The profiles of different diameter of smooth endoplasmic reticulum are observed. Micromark = 1 μm. (d) Mitochondria with swollen cristae (star) and a lipid droplet (Lip). Some profiles of different diameter of smooth endoplasmic reticulum and a multivesicular body (circle) are also seen. Micromark = 1 μm

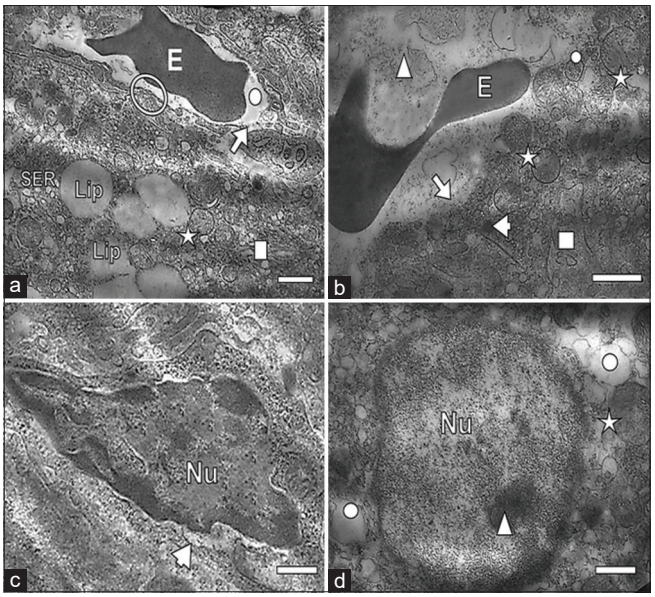

Figure 4: The adrenal gland cortex after 24 h of *Bothrops venezuelensis* venom injection. (a) Inside the capillary, an erythrocyte (E) is seen. The endothelial wall shows some fenestrae (oval), and there is an area of discontinuity of the wall (circle). Several lipid drops (Lip), profiles of smooth endoplasmic reticulum as well as areas lacking smooth endoplasmic reticulum (square) are noticed. Some swollen mitochondria (star) are seen. Micromark = 1 μm. (b) The destruction of a capillary (triangle) is observed. The endothelial wall was lost (arrow). Mitochondria of the cortical cell (star) are appreciated. The multivesicular body (circle), loss of the smooth endoplasmic reticulum (square), and a lysosome (arrow head) are observed. Micromark = 1 μm. (c) The nucleus (Nu) exhibits some areas of the swollen perinuclear space (arrowhead). Micromark = 1 μm. (d) It is observed a nucleus (Nu) without heterochromatin, and a electron dense body that could be the nucleolus but with its characteristic structure lost (fibrillar centre, dense fibrillar component, and granular component) (triangle). The structure of the nuclear envelope is not distinguished, and in the cytoplasm, there is degeneration, with swollen profiles of smooth endoplasmic reticulum (circle). Mitochondria with swollen cristae (star) are observed. Micromark = 1 μm

Table 1: Quantitative analysis of principal component analyses, under *Bothrops venezuelensis* venom actions

B.v venom (time in hours)	Thickening of the capillary endothelium (µm)		Capillary lumen ($µm^2$)		Nucleus area ($µm^2$)		Thickening of perinuclear space (µm)		Number of mitochondria ($µm^2$)		Area of the mitochondria ($µm^2$)		Number of mitochondria cristae		Diameter of the cisternae of the SER (µm)	
	Mean±SD															
3	0.29±0.017	d	8.68±0.10	d	16.08±0.31	ab	1.55±0.080	d	14.88±0.19	ab	0.16±0.012	d	26.60±0.82	a	0.047±0.0085	f
6	0.47±0.012	c	9.98±0.14	b	12.53±0.48	c	1.35±0.092	b	16.33±0.17	bcd	0.30±0.026	c	20.95±0.86	b	0.147±0.0049	e
24	0.81±0.014	a	11.10±0.17	a	8.33±0.43	de	1.08±0.115	a	19.18±0.18	d	0.37±0.025	b	8.98±0.91	d	0.209±0.0104	c
	Control															
3	0.31±0.013	d	8.58±0.08	d	17.28±0.40	a	1.75±0.117	e	14.10±0.13	a	0.14±0.0089	d	27.46±0.74	a	0.011±0.0009	g
6	0.31±0.013	d	8.48±0.08	d	16.93±0.36	ab	1.78±0.121	e	14.00±0.14	a	0.13±0.0082	d	26.21±1.13	a	0.009±0.0008	g
24	0.29±0.014	d	8.78±0.13	d	17.28±0.42	a	1.78±0.127	e	14.10±0.14	a	0.14±0.0086	d	26.62±0.91	a	0.007±0.0005	g

To evaluate the effect of thickening of the capillary endothelium, capillary lumen, nucleus area, thickening of perinuclear space, number of mitochondria, area of the mitochondria, number of mitochondrial cristae, and diameter of the cisternae of the smooth endoplasmic reticulum, an ANOVA of two factors at 95% confidence was developed in which it was found that there were significant differences for changes in the treatments (factor 1) $P=0.00$ and significant difference for times (factor 2) $P=0.00$, with an interaction of $P=0.00$. The table shows the trends of the means and standard deviations for the two treatments over time, obtained during the study of the above parameters. The letters a, b, c, d, e, f, and g are derived from a posteriori SDD, in which the groups that have significant differences, in alphabetical order among their means, and they were given with different letters. The group with the higher mean was defined with the letter a, and when its average significantly decreased, they were assigned and denoted by different letters (a to g)[20]. ANOVA: Analysis of variance, SDD: Smallest statistically detectable difference; SD: standard deviation; *B.v*: *Bothrops venezuelensis*, SER: Smooth endoplasmic reticulum

Table 2: Principal components analyses

	PCA 1	PCA 2
E-values	9.089	0.496
Percentage	90.892	4.962
Accumulated percentage	90.892	95.854

The PCA-1 (X axis of Figure 5) describes 90.89% of the information of the variable system and (PCA)-2 (y axis of Figure 5) 4.9% of this information. The figure as a whole expresses 95.85% of the variables (accumulated percentage) which is considered a satisfactory representation. PCA: Principal component analyses

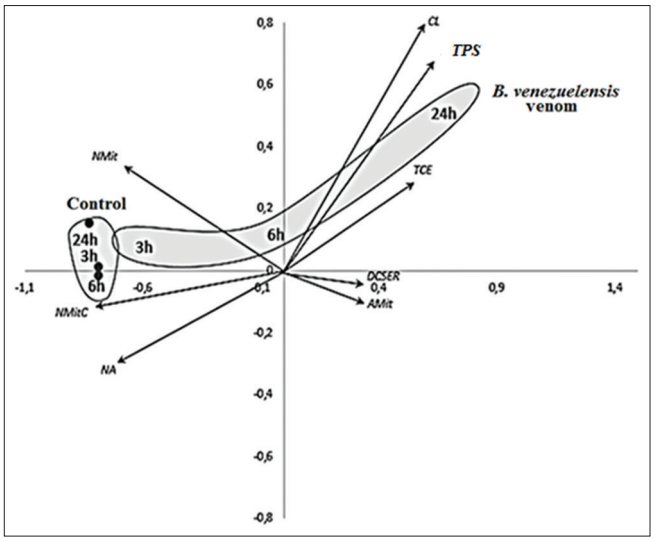

Figure 5: Graphical representation of the principal component analyses. The points describe the temporal performance (3, 6, and 24 h) of the control group and *Bothrops venezuelensis* venom. The points of the coordinate system represent 95.85% of the information synthesized in the eight variables described: Area of the mitochondria (AMit), Number of mitochondria cristae (NMitC), Number of mitochondria (NMit), Area of the nucleus (NA), Diameter of cisternae of the smooth endoplasmic reticulum (DCSER), Thickening of the capillary endothelium (TCE), Capillary lumen (CL), and Thickening of perinuclear space (TPS). The autovectors (E-values) indicate the direction in which each variable (previously described) increases its magnitude

information. The figure as a whole expresses 95.85% of the variables (accumulated percentage).

Table 3 shows the major constituents variables that were correlated. It is observed that there was a high positive correlation between the area of the mitochondria, the diameter of the cisternae of the SER, thickening of the capillary endothelium, capillary lumen, and the perinuclear space in Axis 1 and positive correlation between the number of mitochondria, thickening of the capillary endothelium, capillary lumen, and the perinuclear space in Axis 2.

Figure 5 shows a graphical representation of the PCA. The points describe the temporal performance (3, 6, and 24 h) of the control group and *Bv* venom. The points of the coordinate system represent 95.85% of the information synthesized in the eight variables.

At 6 and 24 h [Tables 1-3 and Figures 5 and 6a], the current study demonstrated that *Bv* venom significantly induced an increase in the thickening of the capillary endothelium, being more intense at 24 h (0.81 μm) (normal = 0.31 μm).

The changes in the capillary lumen appeared 6 h after the venom injection, increasing to 9.98 μm^2 (normal = 8.48 μm). At 24 h, an increase up to 11.10 μm^2 (control = 8.78 μm^2) was observed [Tables 1-3 and Figures 5 and 6b].

The nucleus area only had a significant decrease at 24 h (8.33 μm^2) (normal = 17.28 μm^2) after venom injection, although at 6 h, it had a discrete decrease (12.53 μm^2) (control = 16.93 μm^2) [Tables 1-3 and Figures 5 and 6c].

The perinuclear space at 3 h remains within the parameters of normal control but increased slightly at 6 h (16.33 μm) (control = 14.10 μm), but at 24 h (19.18 μm) (control = 14.0 μm), the rise is higher [Tables 1-3 and Figures 5 and 6d].

The number of mitochondria remained within the parameters of normal control (1.78 mit/analyzed fields), until 24 h (1.08 mit/analyzed fields) when there was a decrease in their number [Tables 1-3 and Figures 5 and 7a].

The mitochondrial area showed at 6 (0.30 μm^2) (normal control = 0.13 μm^2) and 24 h (0.37 μm^2) (normal control = 0.14 μm^2) postinjection of venom that their area increased [Tables 1-3 and Figures 5 and 7b].

Merely, at 24 h, the number of cristae sensibly decreased (8.98 cristae for mitochondria (crist/mit) (normal control 26.62 crist/mit), maintaining normal values at 3 and 6 h [Tables 1-3 and Figures 5 and 7c].

The diameters of the cisternae of the SER showed an increase, at 3 h after the injection of the venom (0.047 μm) (normal

Table 3: Principal component variables

PCV	Axis 1	Axis 2
AMit	0.325	−0.106
NMitC	−0.328	−0.032
NMit	−0.319	0.175
NA	−0.322	−0.208
DSERC	0.325	−0.075
TCE	0.315	0.12
CL	0.301	0.494
TPS	0.316	0.388

The information shows the principal component variables that were correlated. It was observed that there was a high positive correlation between the area of the mitochondria, the diameter of the cisternae of the smooth endoplasmic reticulum, thickening of the capillary endothelium, capillary lumen, and the perinuclear space in Axis 1 and with a correlation positive, between the number of mitochondria, thickening of the capillary endothelium, capillary lumen, and the perinuclear space in Axis 2. PCV: Principal component variables, AMit: Area of mitochondria, NMitC: Number of cristae, NMit: Number of the Mitochondria, NA: Nucleus Area, DSERC: Diameter of cisternae of the smooth endoplasmic reticulum, TCE: Thickening of the capillary endothelium, CL: Capillary lumen, TPS: Thickening perinuclear space

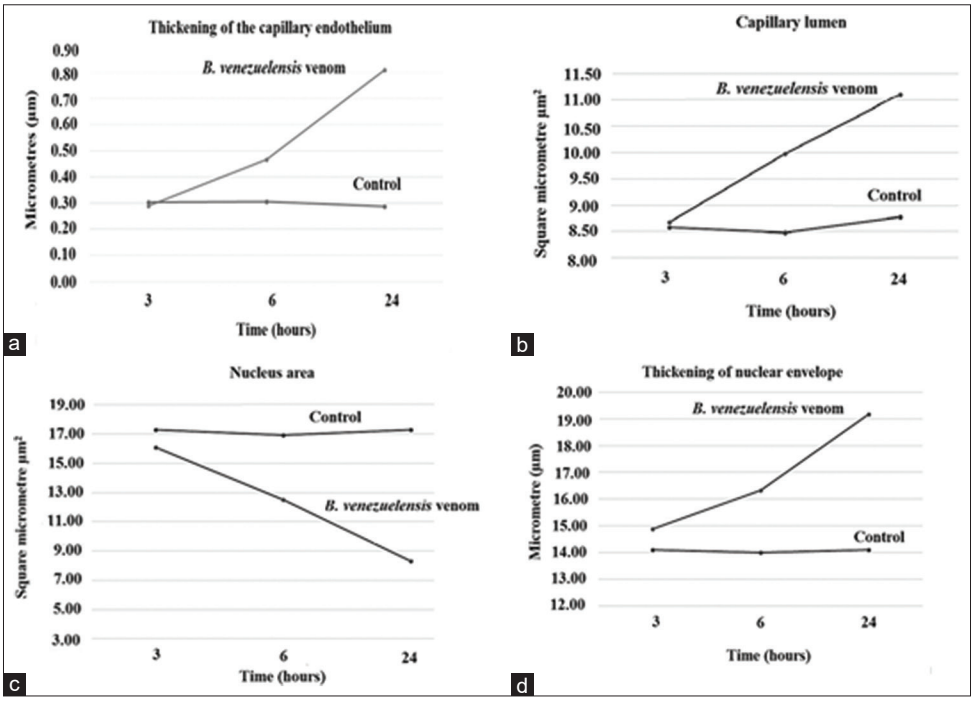

Figure 6: (a) thickening of capillary endothelium, (b) capillary lumen variations, (c) nucleus area changes, and (d) thickening of perinuclear space after 3, 6, and 24 h of *Bothrops venezuelensis* venom injection were evaluated by an analysis of variance of two factors, which was developed at 95% confidence. It was found that there were stastistically significant differences for changes in the treatments (factor 1) $P = 0.00$ and significant difference for times (factor 2) $P = 0.00$, with an interaction of $P = 0.00$. The figure shows the tendencies of the means by the two treatments over time. The values are showed in Table 1

control = 0.011 μm). At 6 h, an intense increase was detected (0.147 μm) (normal control = 0.009 μm) and at 24 h, a higher increase (0.209 μm) (normal control = 0.007 μm) in the diameter of the cisternae was observed [Tables 1-3 and Figures 5 and 7d].

Discussion

The studies in transmission electron microscopy of several organs have allowed describing the alterations caused by the bothropic venoms; however, there are not records on similar studies in the adrenal gland. Therefore, it was decided to study the alterations in this gland, produced by the venom of *Bv*. The adrenal gland is an organ of capital importance for the correct homeostasis equilibrium in mammals throughout the synthesis of mineralocorticoids and glucocorticoids hormones.[21] The endocrine adrenal gland controlling the intensities of cortisol and other vital stress-associated hormones is an essential organ of the hypothalamic–pituitary–adrenal axis (HPA) designated as the body's "stress system."[21,22]

The participation of pituitary–adrenal axis (HPA) in the acute phase of circulatory shock has been confirmed by histopathological validation.[23,24] The adrenal gland cortex is responsible for the production of cortisol, aldosterone, and androgens, which control the electrolyte balance, blood pressure, lipid and glycogen metabolism, and estrogenic biosynthesis[25] is controlled by neuroendocrine hormones, which are originated from the pituitary gland, under the control of the brain hypothalamic region, as well as by the renin-angiotensin system.[26] The biochemical or ultrastructural alterations induced by the toxins of the *Bv* venom can be generated indirectly through the previous system or directly through the adrenal gland. In the present study, it is shown that adrenal cortex injuries induced by *Bv* venom have diverse toxin-pharmacological effects, resulting in important adrenal gland subcellular damages. It could be speculated that by their enzymatic character, mainly the phospholipases and metalloproteases, may be involved in this damage.

In an early period, 3 h after *Bv* venom injection, the adrenal cortex showed swollen SER of cortical cells. The endoplasmic reticulum (ER) damage is caused by disturbances in it structure and function, mainly triggered by glucose deprivation and depletion of Ca^{2+} stores; also produced by the exposure to free radicals, and the accumulation of unfolded or misfolded proteins.[27] This lead to the initiation of a cell stress response, such as the unfolded protein response. As it is known, surface and secreted proteins are synthesized, fold, and assemble before being transported throughout the ER.[27]

In the nucleus, an ultrastructural damage with variable heterochromatin content, irregular edges, and swollen perinuclear space were seen. The nuclear envelope has physical connections to chromatin, via nuclear lamins (Class V intermediate filaments), interacting with membrane-associated

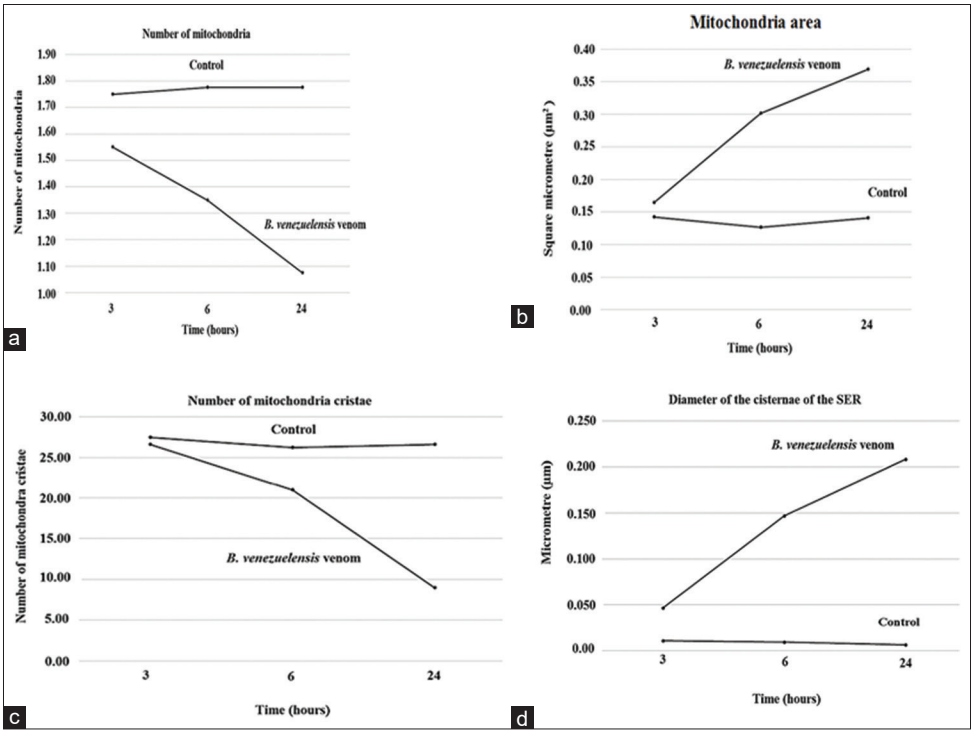

Figure 7: (a) number of mitochondria fluctuations, (b) mitochondria area variations, (c) number of mitochondria cristae, and (d) diameter of the smooth endoplasmic reticulum cisternae after 3, 6, and 24 h of *Bothrops venezuelensis* venom injection were evaluated by an analysis of variance of two factors at 95% confidence. It was found that there were statistically significant differences for changes in treatments (factor 1) $P = 0.00$ and significant difference for times (factor 2) $P = 0.00$, with an interaction of $P = 0.00$. The figure shows the tendencies of the means by the two treatments over time. The values are showed in Table 1

proteins and forming the nuclear lamina on the interior of the nuclear envelope that links straight to chromatin[28] and to chromatin-binding nuclear membrane proteins. The shape of a nucleus is determined by the nuclear lamina, which is closely related with the inner nuclear membrane, and the cytoskeleton. Nevertheless, the way linking the differentiation condition of a cell and the shape variations of its nucleus are not well comprehended. The nuclear-size escalation has been related with nuclear lamina CxxM motif proteins, such as lamins and kugelkern gen.[29,30]

Nuclear envelope is a theorized regulator, of the effects of cellular influences on chromatin or gene expression.[31,32] The exact mechanisms governing the edema of the perinuclear space caused by the toxins of *Bv* are unknown; it is possible that the phospholipases, serine proteases, and metalloproteases may be participating in this damage. A swollen RER cisternae and a pathological autophagic vacuole, with swelling of the mitochondrial cristae, as well as an increase in the swelling of the SER, probably were also produced by the action of phospholipase A_2 (PLA_2).[33] Contrariwise, as it is known, under physiological conditions, autophagy is considered as a normal event, which is required for maintaining a healthy mitochondrial compartment, by the elimination of old and damaged mitochondria.[34]

After 6 h postinoculation with *Bv* venom, the adrenal cortex changes observed at 3 h (swollen SER and nucleus with swollen nuclear envelope) persisted, but now, other ultrastructural changes such as electrondense lipids and mitochondria with swollen cristae as well as a pseudoinclusion in the nucleus with associated heterochromatin were noticed. The myelin figure may be resulting from the dissociation of lipoproteins phosphatide groups, which stimulate the incorporation and intercalation of water between the lamellar stacks of the membranes.[35]

After 24 h postinoculation with *Bv* venom, the adrenal cortex showed a disseminated damage of the capillary vascular system, with a MVB presence. Hemorrhagic metalloproteinases and toxic PLA_2 of *Bv* venom are highly toxic hemorrhagic proteases, degrading endothelia and cleaving plasma proteins, in a relatively specific and nonspecific manner.[3,36]

At 24 h, mitochondrial damage was still evident, with disappearance of cristae and SER. The lesions observed at 3 h were maintained and aggravated after 24 h. This enzymatic cocktail of *Bv* venom proteases together with the phospholipases was undoubtedly the cause of these subcellular alterations. The (ER) has a crucial role in preserving cellular homeostasis, and the MVB development occurs during ER stress, which is induced by the inhibition of ER stress transducers inositol, which requires Inositol-requiring enzyme 1 (IRE1) and PKR-like ER kinase (PERK).[37]

Once the qualitative alterations were established, these results lead us to conclude that there was a statistically significant difference, among the treatments since the value of *P* was less than the significance (α) specified. These values were unlikely to be fortuitous but rather were alterations caused by the *Bv* venom treatment. It was important to demonstrate that these alterations at quantitative level allowed us obtaining information at the different periods studied.

The quantitative analysis showed the morphometric analyses, which was carried out in 100 randomly selected electron micrographs, from each adrenal gland cortex, corroborating whether the action of the venoms had statistical significance.

This quantitative study of PCA, under *Bv* venom activity on thickening of the capillary endothelium, capillary lumen, nucleus area, thickening of nuclear envelope, number of mitochondria, area of the mitochondria, number of mitochondrial cristae, and diameter of tubular elements of the SER were established. The application of the previous method showed good reproducibility and can be used for the demonstration of alterations of these subcellular structures by the venom action.

The current study demonstrated that *Bv* venom, at 6 and 24 h [Table 1], significantly induces an increase in the thickening of the capillary endothelium. It is known that the endothelial cell synthesizes supplies and releases different molecules accomplishing autocrine, paracrine, and endocrine functions. The endothelial membrane has different receptors for physical, chemical, hormonal, and immunological signals, which integrate it into the psychoneuroimmunoendocrine complex. Therefore, the endothelium thickening can produces an alteration, both in the excretion and in its capacity of receptors mentioned above. The highest exposure of the endothelia is probably due to its high dissemination throughout the vascular system of the adrenal gland. Thus, venom activity on various ligands could induce a variety of physiopathological and toxicological reactions, causing several ostensible adrenal toxicities. PLA_2s from *Bothrops* venoms are the leading constituents, liable for cellular damage during the hydrolysis of membrane phospholipids.[38] These abnormalities observed in the capillaries, such as thickening of the endothelium and the presence of prolongations toward its lumen, constitute alterations that occur during bothrophic envenomation, and whose results have been reported by a number of authors.[39,40]

The present study also showed at 6 and 24 h [Table 1] that *Bv* venom induced an increase in the capillary lumen. The relative capillary lumen widening was the first morphologic change observed. Despite the fact that relative capillary area is decreased by the edema, the true capillary lumen was increased. This may be produced by the elevation of blood pressure effect in a blocked capillary when a new flow of blood is streaming from the artery (which could be caused by coagulant proteins of venom).[3]

This work showed that at 6 h, *Bv* venom induced a discrete decrease in the nucleus area [Table 1]. However, at 24 h, the venom caused a significant nuclear decrease. The processes of achievement of *Bothrops* venom nucleus toxicity are not yet explained. Nevertheless, this decrease in nuclear area has been defined as a cellular response to lesions made by pathogens, in

a process known as hypofunction, which consists of a decrease in metabolic activity, and occurs in cases of atrophy.[41] Many venom snake toxins are able to stimulate the production of free radicals, contributing to the inflammatory activities.[42] These mediators are closely associated to the oxidative stress. Nevertheless, nuclear damage by the apoptosis generation may not be discarded. Many authors have described the apoptotic action of different classes of toxins, for instance, metalloproteases and PLA_2s.[42,43]

This study showed that at 6 h, *Bv* venom induced a minor increase in the thickening of the nuclear envelope [Table 1]. However, at 24 h, the increase was higher. The nuclear envelope is constituted of an external nuclear membrane that is continuous to the ER and the pore components. It is structurally and functionally different of the inner nuclear membrane.[44] Thus, it is formed of specific integral membrane proteins and has a clear connection with the underlying lamina.[45,46] Once again, it is thought that the thickening of this membrane could be caused by the action of the proteases and the phospholipases present in the *Bv* venom. Thus, revisions on the mechanism of venom action indicated that the majority of the detected toxic effects possibly result from specific actions of this venom, on the target cell membrane and breaking its integrity, which induces instabilities in cell homeostasis.[46]

The present study also demonstrated that the time of venom exposition (24 h) decreases the average number of mitochondria per cell [Table 1]. Mitochondria frequently change their morphology since they are extremely dynamic organelles. The changes occur to adequate the bioenergetics necessities of the cell, particularly in a state of environmental or metabolic pressures.[33] However, they do not only change their morphology; additionally, they decrease their number under stress situations. In general, the mitochondrial compartment dynamic forces are organized by two contrasting routes, such as mitochondrial fusion and fission.[33] Both increase the production of energy Adenosine triphosphate (ATP) but decrease the number of mitochondria.

Several studies have shown that various toxicological factors inhibit protein synthesis (e.g., cycloheximide), which can induce a high mitochondrial fusion, termed as stress-induced mitochondrial hyperfusion:[47] The mitochondria once fused are further metabolically competent and can deal with augmented energy request through stress circumstances. This persistent stress eventually directs to mitochondrial disintegration and to apoptosis. Both mitochondrial fusion and fission processes can be affected by proteolysis and posttranslational modifications, caused in the current situation by the *Bv* venom proteases. Finally, autophagy, which also decreases the number of mitochondria, is essential for preserving a healthy mitochondrial segment, by removal of old and damaged mitochondria.[33]

Bv venom-induced modifications in the morphology of mitochondria and the mitochondrial matrix come to be cleared due to the swelling. The mitochondrial area was increased at 6 and 24 h postinjection of venom. The normal membrane structure is the requirement for retaining mitochondrial oxidative phosphorylation and ATP formation.[48] Mitochondrial swelling dysfunction directs to reduced oxidative phosphorylation and increased permeability. In the adrenal gland, this could cause a release of proapoptotic factors from the mitochondria, which triggers events for mitochondrial apoptotic signaling.[49,50] These ultrastructural adrenal cortex changes have been described in previous studies caused by the toxin action of *Apis mellifera* venom.[51]

Other micrograph examinations in cells of the cortex adrenal revealed a destruction of mitochondrial cristae exposed to *Bv* venom. The number of cristae sensibly decreased as early as 6 h of venom treatment and extended progressively until 24 h of experiment; its persistence evidences a general incursion of the intracellular membrane systems. After 6 h of venom injection, the number of mitochondrial cristae began to decrease, observing an electron density of the mitochondrial matrices, which can initiate a process of autophagy. Possibly, this deterioration can be due to a cytotoxic Viperidae snake venom effects,[38] which could explain, why these alterations were observed in the case of *Bv* venom. There have been exceptions, particularly in rapidly metabolically active tissues, in which the mitochondria can be large or small and have or lack of cristae. These facts agree with the number of mitochondrial cristae per mitochondrion, and the number of the mitochondria per unit area was apparently unrelated. These mitochondrial alterations coincide with modifications reported in mouse hepatocytes, experimentally envenomed with rattlesnake venom.[52] The manifestation of membrane-degrading enzymes such as venom phospholipases and proteases is advised. The alteration of mitochondrial cristae structure or number is closely related with severe mitochondrial dysfunction. The mitochondria display a fast prompt fall in cytochrome oxidase and a progressively lessening of succinate dehydrogenase.[53] Mitochondria generate more than 90% of the energy required to maintain organ function. When they break down, less energy is produced inside the cell; it is damaged and can still die.

Examining the cisternae of the SER diameters, a light increase was observed at 3 h from venom injection, at 6 h, it was maintained, but at 24 h, an intense increment in the cisternae diameter was noticed. Given the large presence of electro dense lipids observed in the results, we can assume that there was disorganization in the activity of the SER, and based on this assumption, a more detailed study must be focused. SER covers approximately 80% of the adrenal gland and also participates in the process of conversion of pregnenolone to corticosteroids, another reason for the importance of its observation during toxin venom accident.[11] Lloyd *et al.*[54] indicated that the swelling of the cisternae of the ER was not necessarily related to the increased activity. It should be remembered that the toxins present in the snake venoms could imply a process of final mitochondrial degeneration, as was seen previously in the mitochondrial alterations; therefore, this would compromise the production of energy (ATP), adapting

the active transport of ions from the cell membrane and from the sodium–potassium pump; the impact of this is the entry of sodium and water into the cell.[54]

Conclusion

Our experimental work showed a diverse range of effects caused by the *Bv* venom activities. The *Bv* venom acted on subcellular organelles changing the morphology or number of capillaries, endothelia, nucleus, mitochondria, and SER. It appears that these changes were principally caused by the venom proteases and phospholipases and also other components of the venom such as peptides, several enzymes, nonenzymatic toxins, and minerals. All these results advise that adrenal cortex lesions may be significant in the etiopathogenesis of *Bv* snake envenoming. To our knowledge, this is the first report on ultrastructural adrenal gland damages caused by *Bothrops* venom.

Financial support and sponsorship

This work was partially supported by Grant from the Science and Technology Fund (FONACIT) programs (PEI 201400352) (Universidad Central de Venezuela, Dr. A. Rodríguez-Acosta)

Conflicts of interest

There are no conflicts of interest.

References

1. Farsky SH, Gonçalves LR, Cury Y. Characterization of local tissue damage evoked by *Bothrops jararaca* venom in the rat connective tissue microcirculation: An intravital microscopic study. Toxicon 1999;37:1079-83.
2. Girón ME, Guerrero B, Salazar AM, Sánchez EE, Alvarez M, Rodríguez-Acosta A. Functional characterization of fibrinolytic metalloproteinases (colombienases) isolated from *Bothrops colombiensis* venom. Toxicon 2013;74:116-26.
3. Sánchez EE, Girón ME, Uzcátegui NL, Guerrero B, Saucedo M, Cuevas E, *et al*. Biochemical and biological characterisation of lancehead (*Bothrops venezuelensis* Sandner 1952) snake venom from the venezuelan central coastal range. Bol Malariol Salud Ambient 2014;54:138-49.
4. Girón ME, Padrón V, Ramos MI, Sánchez EE, Guerrero B, García A, *et al*. Intraspecies geographical variability in the South American tigra mariposa (*Bothrops venezuelensis* Sandner 1952) snake venom activities. Toxicon 2018;144:23-33.
5. Moura-da-Silva AM, Butera D, Tanjoni I. Importance of snake venom metalloproteinases in cell biology: Effects on platelets, inflammatory and endothelial cells. Curr Pharm Des 2007;13:2893-905.
6. Echeverría S, Leiguez E, Guijas C, do Nascimento NG, Acosta O, Teixeira C, *et al*. Evaluation of pro-inflammatory events induced by *Bothrops alternatus* snake venom. Chem Biol Interact 2018;281:24-31.
7. Mandelbaum FR, Reichel AP, Assakura MT. Isolation and characterization of a proteolytic enzyme from the venom of the snake *Bothrops jararaca* (Jararaca). Toxicon 1982;20:955-72.
8. Zhang Y, Tu AT. The effect of snake venoms and their components on adreno medullary cells: Catecholamine efflux and cell damage. Neurotoxicology 2002;23:273-9.
9. Markland FS Jr., Swenson S. Snake venom metalloproteinases. Toxicon 2013;62:3-18.
10. Aznaurian AV, Amiryan SV. Histopathological changes induced by the venom of the snake *Vipera raddei* (Armenian adder). Toxicon 2006;47:141-3.
11. Sánchez EE, González R, Lucena S, García S, Finol HJ, Suntravat M, *et al*. Crotamine-like from Southern Pacific rattlesnake (*Crotalus oreganus helleri*) Venom acts on human leukemia (K-562) cell lines and produces ultrastructural changes on mice adrenal gland. Ultrastruct Pathol 2018;42:116-23.
12. Salazar E, Salazar AM, Taylor P, Ibarra C, Rodríguez-Acosta A, Sánchez E, *et al*. Pro-inflammatory response and hemostatic disorder induced by venom of the coral snake *Micrurus tener tener* IN C57BL/6 mice. Toxicon 2018;150:212-9.
13. Ribeiro LA, Jorge MT. Bites by snakes in the genus *Bothrops*: A series of 3,139 cases. Rev Soc Bras Med Trop 1997;30:475-80.
14. da Silva Souza A, de Almeida Gonçalves Sachett J, Alcântara JA, Freire M, Alecrim MDGC, Lacerda M, *et al*. Snakebites as cause of deaths in the Western Brazilian Amazon: Why and who dies? Deaths from snakebites in the Amazon. Toxicon 2018;145:15-24.
15. Burke CW. The anterior pituitary, snakebite and Sheehan's syndrome. Q J Med 1990;75:331-3.
16. Proby C, Tha-Aung, Thet-Win, Hla-Mon, Burrin JM, Joplin GF. Immediate and long-term effects on hormone levels following bites by the Burmese Russell's viper. Q J Med 1990;75:399-411.
17. Pifano, F. Investigacion y docencia en Medicina Tropical. Arch Ven Med Trop Parasitol Med 1961;4:1-203.
18. Spearman-Kärber R. Alternative methods of analysis for quantal responses. In: Finney D. editor. Statistical Method in Biological Assay. London: Charles Griffin; 1978. p. 1-78.
19. Milton JS. Estadística para Biología y Ciencias de la Salud. Madrid: Mc Graw-Hill Interamericana; 2001.
20. Angst F, Aeschlimann A, Stucki G. Smallest detectable and minimal clinically important differences of rehabilitation intervention with their implications for required sample sizes using WOMAC and SF-36 quality of life measurement instruments in patients with osteoarthritis of the lower extremities. Arthritis Rheum 2001;45:384-91.
21. Liu JP, Clarke IJ, Funder JW, Engler D. Evidence that the central noradrenergic and adrenergic pathways activate the hypothalamic-pituitary-adrenal axis in the sheep. Endocrinology 1991;129:200-9.
22. Pippal JB, Fuller PJ. Structure-function relationships in the mineralocorticoid receptor. J Mol Endocrinol 2008;41:405-13.
23. Ben-Shlomo A, Mirocha J, Gwin SM, Khine AK, Liu NA. Sheinin RC, Melmed S. Clinical factors associated with biochemical adrenal-cortisol insufficiency in hospitalized patients. Am J Med 2014;127:754-62.
24. Gopalakrishnan M, Vinod KV, Dutta TK, Shaha KK, Sridhar MG, Saurabh S. Exploring circulatory shock and mortality in viper envenomation: A prospective observational study from India. Q J M 2018;111:799-806.
25. Marieb EN, Hoehn K. Human Anatomy and Physiology. 9th ed. San Francisco: Pearson; 2012.
26. Bennett PN, Brown MJ. Clinical Pharmacology. Cambridge UK: Churchill Livingstone; 2008. p. 1-616.
27. Ma Y, Hendershot LM. The unfolding tale of the unfolded protein response. Cell 2001;107:827-30.
28. Moir RD, Spann TP, Goldman RD. The dynamic properties and possible functions of nuclear lamins. Int Rev Cytol 1995;162B:141-82.
29. Prüfert K, Vogel A, Krohne G. The lamin CxxM motif promotes nuclear membrane growth. J Cell Sci 2004;117:6105-16.
30. Brandt A, Papagiannouli F, Wagner N, Wilsch-Bräuninger M, Braun M, Furlong EE, *et al*. Developmental control of nuclear size and shape by Kugelkern and Kurzkern. Curr Biol 2006;16:543-52.
31. Gant TM, Wilson KL. Nuclear assembly. Annu Rev Cell Dev Biol 1997;13:669-95.
32. Burke B, Stewart CL. Life at the edge: The nuclear envelope and human disease. Nat Rev Mol Cell Biol 2002;3:575-85.
33. Youle RJ, van der Bliek AM. Mitochondrial fission, fusion, and stress. Science 2012;337:1062-5.
34. He H, Lu WF, Ke YZ, Zhang YM. An experimental study in etiologic effect of pancreas divisum on chronic pancreatitis and its pathogenesis. World J Gastroenterol 1998;4:533-5.
35. Revel JP, Ito S, Fawcett DW. Electron micrographs of myelin figures of phospholipids simulating intracellular membranes. J Biophys Biochem Cytol 1958;4:495-8.

36. Stocker K, editor. Snake Venom Proteins Affecting Hemostasis and Fibrinolysis in Medical Use of Snake Venom Proteins. Ann Arbor, Boston, Boca Raton Fl: CRC Press; 1990. p. 97-160.
37. Kanemoto S, Nitani R, Murakami T, Kaneko M, Asada R, Matsuhisa K, *et al*. Multivesicular body formation enhancement and exosome release during endoplasmic reticulum stress. Biochem Biophys Res Commun 2016;480:166-72.
38. Marcussi S, Stábeli RG, Santos-Filho NA, Menaldo DL, Silva Pereira LL, Zuliani JP, *et al*. Genotoxic effect of Bothrops snake venoms and isolated toxins on human lymphocyte DNA. Toxicon 2013;65:9-14.
39. Moreira L, Gutiérrez JM, Borkow G, Ovadia M. Ultrastructural alterations in mouse capillary blood vessels after experimental injection of venom from the snake *Bothrops asper* (Terciopelo). Exp Mol Pathol 1992;57:124-33.
40. Pulido-Mendez M, Rodriguez-Acosta A, Finol HJ, Aguilar I, Girón ME. Ultrastructural pathology in skeletal muscle of mice envenomed with *Crotalus vegrandis* venom. J Submicrosc Cytol Pathol 1999;31:555-61.
41. Ghadially FN. Ultrastructural Pathology of the Cell and Matrix. 5th ed. USA: Butterworth-Heinemann; 1997. p. 1-612.
42. Iwanaga S, Suzuki T. Enzymes in snake venoms. In: Lee CY, editors. Handbook of Experimental Pharmacology, Berlin: Springer-Verlag; 1979. p. 61-158.
43. Kang TS, Georgieva D, Genov N, Murakami MT, Sinha M, Kumar RP, *et al*. Enzymatic toxins from snake venom: Structural characterization and mechanism of catalysis. FEBS J 2011;278:4544-76.
44. Gruenbaum Y, Goldman RD, Meyuhas R, Mills E, Margalit A, Fridkin A, *et al*. The nuclear lamina and its functions in the nucleus. Int Rev Cytol 2003;226:1-62.
45. Cohen M, Lee KK, Wilson KL, Gruenbaum Y. Transcriptional repression, apoptosis, human disease and the functional evolution of the nuclear lamina. Trends Biochem Sci 2001;26:41-7.
46. Coulon A, Berkane E, Sautereau AM, Urech K, Rouge P, Lopez A. Modes of membrane interaction of a natural cysteine-rich peptide: Viscotoxin A3. Biochim Biophys Acta 2002;1559:145-59.
47. Tondera D, Grandemange S, Jourdain A, Karbowski M, Mattenberger Y, Herzig S, *et al*. SLP-2 is required for stress-induced mitochondrial hyperfusion. EMBO J 2009;28:1589-600.
48. Sureda FX, Escubedo E, Gabriel C, Comas J, Camarasa J, Camins A. Mitochondrial membrane potential measurement in rat cerebellar neurons by flow cytometry. Cytometry 1997;28:74-80.
49. Alway SE, Siu PM. Nuclear apoptosis contributes to sarcopenia. Exerc Sport Sci Rev 2008;36:51-7.
50. Marzetti E, Hwang JC, Lees HA, Wohlgemuth SE, Dupont-Versteegden EE, Carter CS, *et al*. Mitochondrial death effectors: Relevance to sarcopenia and disuse muscle atrophy. Biochim Biophys Acta 2010;1800:235-44.
51. Rodríguez-Acosta A, Vega J, Finol HJ, Pulido-Mendez M. Ultrastructural alterations in cortex of adrenal gland caused by the toxic effect of bee (*Apis mellifera*) venom. J Submicrosc Cytol Pathol 2003;35:309-14.
52. Rodriguez-Acosta A, Pulido-Mendez M, Finol HJ, Girón ME, Aguilar I. Ultrastructural changes in liver of mice envenomed with *Crotalus vegrandis* venom. J Sub Cyt Pathol 1999;31:433-9.
53. Toury R, Boissonneau E, Stelly N, Dupuis Y, Berville A, Perasso R. Mitochondria alterations in Cd2+-treated rats: General regression of inner membrane cristae and electron transport impairment. Biol Cell 1985;55:71-85.
54. Lloyd R, Douglas B, Young W. Adrenal gland. Endocrine disease. In: King D, editor. Atlas of Non-Tumor Pathology. Washington D.C: AFIP; 2002. p. 209-12.